Marquette University

e-Publications@Marquette

Mechanical Engineering Faculty Research and Publications

Mechanical Engineering, Department of

8-2001

Multidirectional Compliance and Constraint for Improved Robotic Deburring. Part 2: Improved Bracing

Joseph M. Schimmels
Marquette University, joseph.schimmels@marquette.edu

Follow this and additional works at: https://epublications.marquette.edu/mechengin_fac

Part of the Mechanical Engineering Commons

Recommended Citation

Multidirectional compliance and constraint for improved robotic deburring. Part 2: improved bracing

Joseph M. Schimmels
Department of Mechanical and Industrial Engineering, Marquette University, Milwaukee, WI

Abstract

This two-part paper presents a method for both improving the positioning capability and increasing the effective stiffness (bracing) of a robotic manipulator through multidirectional compliance and constraint. Improved positioning and improved bracing are attained through the effective use of multiple unilateral kinematic constraints in different directions. The companion paper identified how to specify the compliant characteristics of a manipulator so contact forces lead to deflections that eliminate positional misalignments and result in improved relative positioning through force guidance. In this part, we show that the characteristics beneficial to force guidance are the same characteristics that provide improved bracing when partially constrained by contact. Improved bracing is demonstrated in the context of workpart edge deburring.

Keywords

1. Introduction

As presented in the companion paper [1], accurate *relative* positioning can be attained and maintained through the effective use of compliance and constraint. Here, we demonstrate that the form of compliance that improves a manipulator's positioning ability is the same form of behavior that improves its ability to maintain jig–workpart contact despite finite force disturbances.

The effective use of compliance and constraint in robotic material removal is demonstrated here for edge deburring. The surfaces adjacent to the workpart edge are used as reference surfaces whose intersection defines the edge of the workpart. Contact between these reference surfaces and the elements of a properly designed end-effector mounted jig establishes a workpart-edge-based reference frame to which a material removal tool is attached. An example of the use of compliance and constraint in deburring is illustrated in Fig. 1 of the companion paper [1].
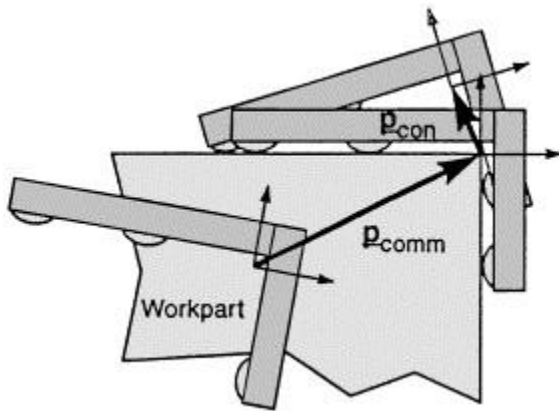

Fig. 1. Commanded and Constrained Deflections. The commanded deflection $\Delta\bar{x}_{comm}$ is the deflection of the compliance from its commanded position. The constrained deflection $\Delta\bar{x}_{con}$ is the deflection of the compliance from its properly constrained position. Here only the translational component $\bar{p}$ of each is illustrated.

To ensure that accurate relative positioning is maintained in a material removal task, the manipulator must reject forces generated by tool–workpart interaction. By achieving unilateral contact with the workpart and "preloading" the compliance, the manipulator end-effector is "braced" to increase the effective end-point stiffness of the manipulator. Through manipulator bracing, material removal disturbance forces result in no end-effector deflection when the force preload is not exceeded or in much smaller deflections when the preload is exceeded.

As demonstrated in the companion paper [1], a compliance with the specified form of directional coupling behavior is best for attaining and maintaining accurate positioning despite positioning errors. Here, we show that the specified form of directional coupling is also beneficial in maintaining accurate positioning by better rejecting the forces that are generated in the material removal process.

1.1. Background
This paper addresses improved bracing through the use of multidirectional compliance and constraint. The benefits associated with the proposed concepts are demonstrated in robotic edge material removal tasks for which accurate relative positioning and rejection of tool–workpart interaction forces are important.

In previous work involving manipulator–workpart interaction, others [2], [3] have addressed the use of kinematic constraint to brace and stiffen the manipulator when removing material. In their work, bracing was accomplished by a single point of contact between the manipulator and the environment. In the proposed work, multiple points of contact and directional coupling in the compliance are used to increase the bracing effect in a *multidimensional* context.

In this work, the *compliance* of the manipulator is specified. Compliance, here refers to the spring-like characteristics of the manipulator *admittance*. Admittance refers to a manipulator's mapping of forces to motions — the inverse of the manipulator impedance [4]. Often, when considering multidirectional mechanical behavior, a diagonal matrix is used to identify the behavior along specified axes at a particular coordinate frame — the *center* of compliance. In the compliance specification algorithm presented in the companion paper, the compliance matrix attained does not, in general, behave as a compliance center. Here, we show that the directional coupling behavior not found in a compliance center is beneficial in increasing the effective stiffness of a partially constrained (braced) manipulator.

In this work, the behavior of a unilaterally *constrained* multidirectional compliance is investigated. Previously, others [5], [6], [7], [8] have investigated the behavior of an *unconstrained* multidirectional compliance. It is shown here that the compliance and the constraint together dictate the overall performance of the manipulator in material removal tasks.

1.2. Compliance control law

A compliance control law is used in this application. As presented and discussed in the companion paper, the linear compliance control law is given by

(1)

$$\delta\bar{x} = \bar{\bar{C}}\bar{f}$$

where $\bar{\bar{C}}$ is the $N \times N$ manipulator compliance matrix, a multidimensional linear mapping of forces to deflections; $\delta\bar{x}$ is the small translational/orientational deflection (a twist [9]) of the manipulator from its commanded ("nominal", "unconstrained", or "virtual") position and orientation; and $\bar{f}$ is the force and torque (wrench [9]) acting on the manipulator.

Note that, for compliance, contact is maintained by the deflection from the commanded position/orientation (i.e., forces are positive only if the commanded position corresponds to geometrical conflict between jig and workpart).

1.3. Overview

This paper introduces the concept of using multidimensional compliance and constraint in robotic material removal applications and illustrates the associated benefits of the concept, improved relative positioning and improved bracing. Jig–workpart contacts are used to provide unique relative positioning with respect to the workpart edge, and the compliance of the manipulator is used to ensure that the unique relative positioning is maintained despite small finite positional error and finite force disturbances.

Section 2 identifies how the effective stiffness of the manipulator is increased through multidirectional bracing. Unilateral contact and compliance preload are used together with the directional coupling in the compliance to reject forces associated with material removal. The properties and terms used in quantifying improved bracing are defined. The calculations used in evaluating these properties when unconstrained, partially constrained, and completely constrained are identified.

In **Section 3**, the improved bracing attained using the prescribed directional coupling in the compliance matrix is demonstrated with the same three matrices in the same three degree-of-freedom positioning example used in the companion paper [1].

Section 4 provides a summary and discussion of results and a brief overview of the direction of future work.

2. Improved bracing

By establishing multiple points of contact, the manipulator is braced in multiple directions to better reject material removal forces that could cause the jig to lose its desired relative positioning. The effective stiffness of the manipulator is increased by compliance preload (for which the external force is, in effect, reduced in magnitude) and partial constraint (for which the deflection is modified by unilateral kinematic constraint).

First, concepts useful in evaluating the effectiveness of a brace in a multidirectional context are developed. A general procedure for calculating the constrained deflection that results from an externally applied force is presented.

2.1. Definitions

The directional variation in compliance is often represented by a compliance ellipsoid to assist in developing a physical appreciation of a compliance matrix. This representation, however, is not useful when the compliance is unilaterally constrained. A means of assessing the effective brace (or reduction in the effective compliance) resulting from contact is considered here.

In previous work by West [10], the *essential compliance* was defined to be the measure of deflection in the direction of the applied force (for which the diagonal elements of the compliance matrix are deemed essential). Here, since deflection in any direction causes loss of unique relative positioning, we define a new term that considers the actual deflection of the jig.

2.1.1. Effective compliance

The effective compliance is defined here as the magnitude of the translational deflection of a point on a body that results from a unit force applied at that point. The location of that point determines, in part, the magnitude of the deflection. Here, in this deburring example, it is chosen to be the location where the deburring tool contacts the workpart — the location at which the disturbance force is applied as illustrated in **Fig. 1** of the companion paper [1]. The *effective compliance*, $\mathbf{C}_{eff}$ is defined by

(2)

$$C_{eff} = \Delta \bar{x} / \bar{f}_e$$

where $\Delta \bar{x} = [\bar{p}^T, \Delta \theta \bar{r}^T]$ as described in [1], for our purposes, its magnitude is the magnitude of the translational deflection $\Delta \bar{x}^2 = \bar{p}^T \bar{p}$; and $\bar{f}_e$ is the magnitude of an externally applied wrench. Since $\tau = \bar{0}$ at the point of the applied force, $\bar{f}_e{}^2 = \bar{f}_e{}^T \bar{f}_e$.

The variation of this measure with varying direction of applied force is investigated. The directionally dependent effective compliance is represented with a vector:

(3)

$$\bar{C}_{eff} = C_{eff} \hat{\bar{f}}_e = \Delta \bar{x} \bar{f}_e \hat{\bar{f}}_e$$

where $\hat{\bar{f}}_e$ is a unit applied wrench in the direction of $\bar{f}_e$, $\hat{\bar{f}}_e{}^T \hat{\bar{f}}_e = 1$. The effective compliance indicates the magnitude of the deflection caused by a unit force in the specified direction.

Related to the effective compliance is the effective brace.

2.1.2. Effective brace

The *effective brace*, $\mathbf{B}_{\text{eff}}$, is defined to be the normalized reduction in the effective compliance due to the constraint

(4)

$$B_{\text{eff}} = C_{\text{eff}_{\text{unc}}} - C_{\text{eff}_{\text{con}}} \, C_{\text{eff}_{\text{unc}}}.$$

This also varies as a function of the direction of the applied force and is similarly represented with a vector:

(5)

$$\bar{B}_{\text{eff}} = C_{\text{eff}_{\text{unc}}} - C_{\text{eff}_{\text{con}}} \, C_{\text{eff unc}} \hat{\bar{f}}_e = \Delta \bar{x}_{\text{unc}} - \Delta \bar{x}_{\text{con}} \Delta \bar{x}_{\text{unc}} \hat{\bar{f}}_e$$

where $C_{eff_{unc}}$ is the unconstrained effective compliance, and $C_{eff_{con}}$ is the constrained effective compliance. The constrained deflection, $\Delta \bar{x}_{\text{con}}$ is the deflection of the jig from its constrained location (the translational component $\bar{p}_{\text{con}}$ is illustrated in **Fig. 1**). The magnitude of the constrained deflection is given by $\Delta \bar{x}_{\text{con}}{}^2 = \bar{p}_{\text{con}}{}^T \bar{p}_{\text{con}}$.

The effective brace indicates the degree to which unilateral contact reduces the deflection that results from a unit force in the specified direction.

2.2. Calculations

The procedures needed to calculate effective compliance for no constraint, partial constraint, and complete constraint are provided below.

2.2.1. Unconstrained effective compliance

As described above, the unconstrained compliance serves as a reference in assessing the effective brace. The unconstrained deflection calculated using **Eq. (18)** of the companion paper [1] is given as

(6)

$$\Delta \bar{x}_{\text{unc}} = \bar{\bar{C}} \bar{f}_e.$$

Therefore, the unconstrained compliance in direction $\hat{\bar{f}}_e$ is

(7)

$$C_{\text{eff unc}} = \bar{\bar{C}} \bar{f}_e / \bar{f}_e.$$

2.2.2. Constrained effective compliance

For the constrained case considered below, the deflection from its constrained position at the workpart edge, as illustrated in **Fig. 1**, for any specified preload is obtained with the procedure provided below. A freebody diagram of the jig, which illustrates the forces that act on it that could lead to deflection from its proper position, is shown in **Fig. 2**.

1. First determine whether the jig is actually constrained in its proper position for the commanded deflection. To do this, calculate the preload force using the commanded geometric interference and the compliance as

   (8)

$$f_p = -\bar{\bar{C}}^{-1}\Delta\bar{x}_{comm}$$

where $\bar{f}_p$ is the preload force — the wrench provided *by* the compliance that results from the commanded deflection, $\Delta\bar{x}_{comm}$. To confirm that the commanded deflection yields a properly positioned jig when no external force is applied, contact forces must, as in Section 3.2.2 of the companion paper, be nonnegative (i.e., contact wrenches are directed out of the workpart):

(9)

$$\phi_p = -\bar{\bar{W}}^{-1}\bar{f}_p \geq 0.$$

The jig is not constrained in its proper position for the commanded deflection if this condition is not satisfied.

2. Next, calculate the constrained deflection from its proper position relative to the workpart edge, $\Delta\bar{x}_{con}$, using the following optimization:[1]

(10)

$$\text{minimize}(\Delta\bar{x}_{comm} + \Delta\bar{x}_{con})^T \bar{\bar{C}}^{-1}(\Delta\bar{x}_{comm} + \Delta\bar{x}_{con})$$

(11)

$$\text{subject to } \bar{\bar{W}}^T \Delta\bar{x}_{con} \geq 0)$$

(12)

$$-\bar{\bar{W}}^{-1}(\bar{f}_e - \bar{\bar{C}}^{-1}(\Delta\bar{x}_{comm} + \Delta\bar{x}_{con})) \geq 0.$$

The constrained deflection resulting from the externally applied force obtained using this procedure: (1) ensures that the *work* performed by the constraint wrenches is nonnegative (Eq. (11)); and (2) ensures that the constraint wrench *magnitudes* remain directed out of the workpart (remain nonnegative) (Eq. (12)). The second constraint equation enforces the fact that contact at each element is unilateral and therefore is not capable of pulling the jig into position. The set of linear inequalities associated with these constraint conditions define a polyhedral convex cone of possible solutions (a very large set of solutions). The actual deflection is the one having the least potential energy. Potential energy provides a useful metric in evaluating the magnitude of deflections involving both translation and rotation.

The constrained compliance in direction $\hat{\bar{f}}_e$ is

(13)

$$C_{eff\,con} = \Delta\bar{x}_{con}/\bar{f}_e$$

where $\Delta\bar{x}_{con}$ is obtained using the optimization procedure described in , , .
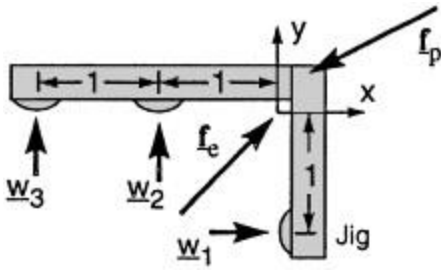
Fig. 2. Three-Point Contact Jig Free Body Diagram. The preload force $\bar{f}_p$, the external (deburring) force $\bar{f}_e$, and the contact forces on the jig locators $\bar{w}_I$,i=1,2,3, are illustrated.

Because deflections are finite, error exists in the linear approximations considered here. However, if rotational deflections are small, associated errors are also small.

2.2.3. Complete constraint

In application, the compliance will be preloaded to ensure accurate positioning and further improve bracing. Before deflection from its constrained position can occur along an axis of unilateral kinematic constraint, the external force applied to a manipulator along that axis must exceed the compressive force exerted on the workpart by the manipulator (i.e., must exceed the preload). Therefore, to provide complete constraint to a known external force, the geometrical interference must provide a preload force, $\bar{f}_p$, greater than the externally applied force, $\bar{f}_e$ in the direction of $\bar{f}_e$.

Similar to that generated in the companion paper, a space of deflections, X, from the properly mated position and orientation that will reject a known external force can be constructed. Deflection from the properly mated position and orientation can only occur if the balance of forces from the preload ($\bar{f}_p = -\bar{\bar{C}}^{-1}\Delta\bar{x}_{comm}$), the workpart contact ($\bar{f}_w = \bar{\bar{W}}\varphi$), and the external force ($\bar{f}_e$) indicates that contact wrenches are negative. The space of acceptable commanded deflections that provide complete constraint to force $\bar{f}_e$ is defined by those commanded deflections that maintain positive contact forces despite the externally applied force. Similar to Eq. (21) in the companion paper, the space of acceptable deflections that maintain contact is a PCC now defined by

(14)

$$(\bar{\bar{C}}\bar{\bar{W}})^{-1}\Delta\bar{x}_{comm} \geqslant \bar{\bar{W}}^{-1}\bar{f}_e$$

where $\Delta\bar{x}_{comm}$ is the commanded deflection from the jig properly mated position.

The space of deflections from the properly mated position and orientation, X, that will reject an external force of known magnitude, $\bar{f}_e$, but arbitrary direction can also be constructed.

(15)

$$(\bar{\bar{C}}\bar{\bar{W}})^{-1}\Delta\bar{x}_{comm} \geqslant \bar{\bar{W}}^{-1}\bar{f}_e \forall \bar{f}_e \bar{f}_e{}^T\bar{f}_e = \bar{f}_e{}^2,$$

(16)

$$(\bar{\bar{C}}\bar{\bar{W}})^{-1}\Delta\bar{x}_{comm} \geqslant \hat{\bar{f}}_e \bar{\bar{W}}^{-1}\hat{\bar{f}}_e \forall \hat{\bar{f}}_e \hat{\bar{f}}_e{}^T\hat{\bar{f}}_e = 1.$$

This condition is, in essence, the intersection of an infinite number of PCCs. The intersection must satisfy the worst case for each row (maximum values in $\bar{\bar{W}}^{-1}\hat{\bar{f}}_e$). The maximum value for each row is obtained when $\hat{\bar{f}}_e$ and $\bar{w}_I{}^{-1}$ are "aligned" (in the same translational direction), where $\bar{w}_I{}^{-1}$ is the ith row of $\bar{\bar{W}}^{-1}$. This yields

(17)

$$(\bar{\bar{C}}\bar{\bar{W}})^{-1}\Delta\bar{x}_{comm} \geqslant \bar{f}_e \sum j=1L(w_{1j}^{-1})^2 : \sum j=1L(w_{Mj}^{-1})^2$$

where w_{ij}^{-1} is the element in the ith row and jth column of $\bar{W}^{-1}$; and L is the number of translational elements in $\bar{f}_e$.

3. Demonstration of improved bracing

The analysis procedure derived above for evaluating the bracing characteristics of a manipulator is demonstrated with the three-degree-of-freedom example considered in the companion paper [1]. The improved bracing performance associated with directional coupling is shown using the same compliance matrices. The unconstrained, partially constrained, and completely constrained behavior of the compliance matrices with varying types of directional coupling are addressed below. The three matrices are

$$\bar{\bar{C}}_d=\bar{\bar{I}},$$

$$\bar{\bar{C}}_{mar}=3-3-2-353-232,$$

$$\bar{\bar{C}}_{max}=2.86-2.82-1.89-2.823.802.84-1.892.842.21.$$

3.1. No constraint

Consider a unit external wrench acting at the origin of task coordinate frame[2] that acts along the direction that we anticipate receiving the largest material removal forces, $\hat{f}_e=[2/2,2/2,0]^T$.

The unconstrained deflection is calculated using Eq. (6). For the decoupled matrix, the unconstrained deflection in this direction is: $\Delta\bar{x}_{unc\,d}=[2/2,2/2,0]^T$. For the compliance matrix that marginally satisfies the conditions for force assembly, the unconstrained deflection in this directions is $\Delta\bar{x}_{unc\,mar}=[0,2,2/2]^T$.

Since the magnitude of the translational component of the deflection $\Delta\bar{x}_{unc\,mar}$ is a factor of 2 larger than that for $\Delta\bar{x}_{unc\,d}$, equivalent magnitude unconstrained deflection can be obtained if the $\bar{\bar{C}}_{mar}$ matrix is appropriately scaled. The coupled matrix, $\bar{\bar{C}}_c$, used subsequently refers to

(18)

$$\bar{\bar{C}}_c=12\bar{\bar{C}}_{mar}.$$

The compliance matrix that will ensure force assembly for friction close to the maximum can be similarly scaled so that the unconstrained translational deflection resulting from a force in this direction has the same magnitude as those obtained with the other matrices. The scaled matrix is given by

(19)

$$\bar{\bar{C}}_m=1.4419\bar{\bar{C}}_{max}.$$

The magnitudes of the translational component of the unconstrained deflection in response to external force input $\hat{f}_e=[2/2,2/2,0]^T$ direction for the compliance matrices are equal to each other: $\Delta\bar{x}_{unc_d}=\Delta\bar{x}_{unc\,c}=\Delta\bar{x}_{unc\,m}=1$. Also, since unit translational deflection resulted from unit force input, the unconstrained compliance in this direction for each matrix is $C_{eff\,unc\,d}=C_{eff\,unc\,c}=C_{eff\,unc\,m}=1$.

By scaling the matrices in this way, the unconstrained deflection for each matrix is the same in the most likely direction of force disturbance. This also establishes a reference, used subsequently, for evaluating constrained compliance.

3.2. Partial constraint without preload

For the case without preload, the jig is nominally positioned exactly on the workpart edge with no compression of the compliance (i.e., $\Delta\bar{x}_{comm}=0$).

3.2.1. Single direction evaluation

The constrained deflection calculated using the procedure outlined in Section 2.2.2 yields a constrained deflection that is equal to the unconstrained deflection for $\bar{\bar{C}}_d$ and $\bar{\bar{C}}_c$ in the given direction of applied force (along a 45° angle from edge):

(20)

$$\Delta\bar{x}_{con\,d}=22,22,0\,^T=\Delta\bar{x}_{unc\,d},$$

(21)

$$\Delta\bar{x}_{con\,c}=0,1,12\,^T=\Delta\bar{x}_{unc\,c}.$$

However, for $\bar{\bar{C}}_m$, the constrained and unconstrained deflections are significantly different

(22)

$$\Delta\bar{x}_{con\,m}=0.2305,0,0\,^T\neq\Delta\bar{x}_{unc\,m}=[0.0408,0.9992,0.9686]\,^T.$$

The effective constrained compliance values in this direction for these matrices with these constraints are calculated using Eq. (2) as: $C_{eff\,con\,d}=C_{eff\,con\,c}=1$ and $C_{eff\,con\,d}=0.2305$.

The effective brace (calculated using Eq. (4)) for $\bar{\bar{C}}_d$ and $\bar{\bar{C}}_c$ in the given direction of applied force is $B_{eff\,d}=B_{eff\,c}=0$. This indicates that the jig is not braced in this direction by contact.

The effective brace in this direction for $\bar{\bar{C}}_m$, however, is significant: $B_{eff\,m}=0.7695$. This indicates that the magnitude of the constrained deflection is almost 77% less than the unconstrained deflection for a force provided along this axis!

3.2.2. General evaluation

To better understand the behavior attained with directional coupling, a general evaluation of external forces is considered. The procedures illustrated above have been programmed to evaluate effective compliance and effective bracing behavior for a force acting at the specified point (the point of tool/workpart contact) in any direction.

Fig. 3 illustrates the directional variation in the constrained and unconstrained effective compliance for the three example compliance matrices. The dashed circle in Fig. 3a illustrates the isotropic behavior associated with the unconstrained directionally decoupled compliance matrix ($\bar{\bar{C}}_d=\bar{\bar{I}}$) and the solid line illustrates its effective compliance with constraint. The dashed line in Fig. 3b illustrates the anisotropic behavior of the directionally coupled compliance matrix $\bar{\bar{C}}_c$ (given in Eq. (18)) and the solid line its effective compliance with constraint. Note that the effective compliance is reduced along axes that are not constrained without the compliance. Fig. 3c illustrates the very anisotropic behavior associated with a compliance matrix that provides large directional

coupling $\bar{\bar{C}}_m$ (given in Eq. (19)). The effective compliance is reduced in all directions when this high degree of directional coupling is present in the compliance matrix.
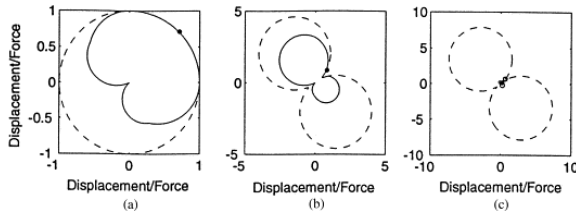

Fig. 3. Comparison of the Directional Variation in the Effective Unconstrained and Constrained Compliance for Example Matrices. In each figure the dashed line identifies the unconstrained compliance and the solid line, the constrained compliance. Fig. 2a was generated using the example decoupled compliance matrix, $\bar{\bar{C}}_d$; Figs 2b and c were generated using an increasing amount of directional coupling, using $\bar{\bar{C}}_c$ and $\bar{\bar{C}}_m$, respectively.

Also shown in each figure are the results of the effective compliance for external force input in the $\hat{\bar{f}}_e = [2/2, 2/2, 0]^T$ direction (calculated in Section 3.2.1). The effective constrained compliance is indicated with a solid dot, and the effective unconstrained compliance is indicated with an open dot along a 45° angle from the origin in each figure. Only for $\bar{\bar{C}}_m$ are the different dots not superimposed, indicating a nonzero effective brace along this direction for this matrix (as calculated).

Fig. 4 better illustrates the comparison of the effective constrained compliance for the decoupled matrix $\bar{\bar{C}}_d$ and the matrix with large directional coupling $\bar{\bar{C}}_m$. This figure shows the significant reduction in the effective compliance due to the specified coupling in the compliance matrix. As shown here, through directional coupling, the effective stiffness of the manipulator is increased *even without preload*. As in Fig. 3, the effective constrained compliance for external force input in the $\hat{\bar{f}}_e = [2/2, 2/2, 0]^T$ direction is indicated with a solid dot for each compliance.
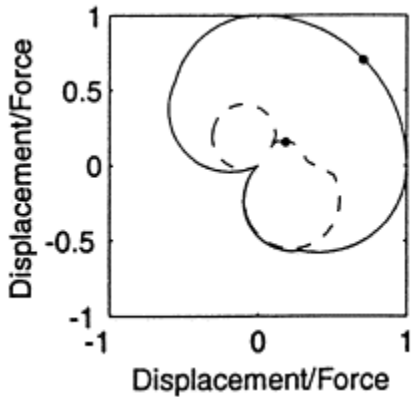

Fig. 4. Directional Variation of the Constrained Effective Compliance for $\bar{\bar{C}}_d$ and $\bar{\bar{C}}_m$. The solid line identifies the constrained effective compliance for the example decoupled compliance matrix $\bar{\bar{C}}_d$, and the dashed line identifies the constrained effective compliance for the compliance matrix with large directional coupling $\bar{\bar{C}}_m$.

Fig. 5 illustrates the comparison of the effective brace, $\bar{B}_{eff}$, for the example matrices. Recall that the effective brace, as defined in Eq. (5), indicates the normalized reduction in the unconstrained compliance that results from constraint. As shown, the coupled matrices provide a significantly larger effective brace in the unconstrained directions when only partially (unilaterally) constrained. The effective brace for external force input in the $\hat{\bar{f}}_e = [2/2, 2/2, 0]^T$ direction is indicated with a solid dot for each compliance.
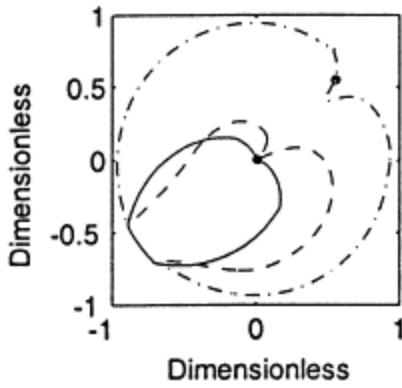
Fig. 5. Directional Variation of the Effective Brace Provided by Multidirectional Constraint. The solid line, the dashed line and the dash-dot line identify the effective brace for the example decoupled compliance matrix $\bar{\bar{C}}_d$, the example coupled compliance matrix $\bar{\bar{C}}_c$, and a compliance matrix with increased directional coupling $\bar{\bar{C}}_m$, respectively.

3.3. Complete constraint with preload

To determine the space of deflections from the properly mated position and orientation that will reject any external force of magnitude of half a unit ($\bar{f}_e$=0.5 force units) acting at the point of tool/workpart contact, Eq. (17) must be satisfied. Since, in this example, $L = 2$ and

$$\bar{\bar{W}}^{-1}=100-1211-1-1$$

Eq. (17) becomes

(23)

$$(\bar{\bar{C}}\bar{\bar{W}})^{-1}\Delta\bar{x}_{comm}\geqslant 12152.$$

Next, the space of acceptable translational deflections from the properly mated position is obtained by intersecting the PCC of Eq. (23) with the $\Delta\theta = 0$ surface (as in Section 4.1 of the companion paper [1]).

The space of acceptable translational deflections that maintain the proper positioning despite an arbitrarily directed half unit force acting at the point of tool/workpart contact is illustrated in Fig. 6 for each of the example compliance matrices. This space is very similar to the space of nominal positions that provides accurate relative positioning discussed in Section 4 of the companion paper [1]. In fact, Fig. 4 of that paper can be viewed as the space of nominal positions that will reject forces of zero magnitude yet maintain accurate relative positioning. As the magnitude of the external force increases, the corresponding space of commanded deflections providing complete constraint for each matrix is shifted down and to the left. As in accurate relative positioning, directional coupling increases the space of acceptable nominal positions that will reject externally applied forces.
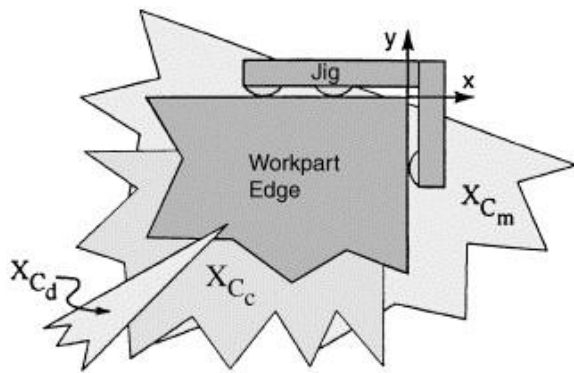
Fig. 6. Space of Acceptable Translational Deflections that Totally Reject a Force of One Half Unit Magnitude. The space of commanded translational deflections that will maintain desired positioning despite any force of half unit magnitude that is arbitrarily directed but acts at the point of tool–workpart contact is illustrated for the 3 example matrices. As the relative amount of directional coupling increases, the space of acceptable commanded deflections that rejects the external force increases (i.e., $X_{C_d} \subset X_{C_c} \subset X_{C_m}$).

Although the unconstrained compliance for the matrices with specified directional coupling is greater than the unconstrained compliance of the decoupled matrix in almost all directions (as shown in **Fig. 3**), the constrained compliance with preload is effectively zero! Therefore, the effective stiffness of the manipulator is dramatically increased when it is both constrained and is described by a compliance matrix of the specified form. The increase in the effective brace — the reduction in the compliance due to contact — is dramatic.

4. Summary and conclusions

This paper has presented a means of accurately tracking a workpart edge despite finite manipulator inaccuracy. In this work: (1) the physical constraints of the task environment are used to provide relative positional information of the manipulator end-effector with respect to the workpart, and (2) the compliance of the manipulator is programmed to provide both external force rejection and positional error correction while tracking these constraints.

The improved bracing behavior associated with the specified direction coupling was demonstrated using a three degree of freedom relative positioning example. The performance of matrices with varying degrees of the specified coupling was compared with that of a compliance "center". The directionally coupled matrices provided a significantly improved rejection of disturbance forces.

Current work addresses how to exactly realize a spatial compliance matrix having the coupling characteristics in a compact mechanism.

References

1. J.M. Schimmels. **Multidirectional compliance and constraint for improved robot deburring: Part 1 — improved positioning.** *Robotics Comput Intergrated Manuf*, 17 (4) (200), pp. 277-286
2. West H, Asada H. Kinematic analysis and mechanical advantage of manipulators constrained by contact with the environment. Proceedings of the ASME Winter Annual Meeting, 1985.
3. Delson N, West H. Bracing to increase the natural frequency of a manipulator: analysis and design. Int J Robotics Res 1993;12(6).
4. N. Hogan. **Impedance control: an approach to manipulation.** *ASME J Dyn Systems Meas Control*, 107 (3) (1985), pp. 1-23
5. Loncaric J. Geometrical analysis of compliant mechanisms in robotics. PhD thesis, Harvard University, 1985.

6. J. Loncaric. **Normal forms of stiffness and compliance matrices.** *IEEE J Robotics Automat*, 3 (6) (1987), pp. 567-572
7. T. Patterson, H. Lipkin. **A classification of robot compliance.** *ASME J Mech Des*, 115 (3) (1993), pp. 581-594
8. T. Patterson, H. Lipkin. **Structure of robot compliance.** *ASME J Mech Des*, 115 (3) (1993), pp. 576-580
9. R.S. Ball. A treatise on the theory of screws, Cambridge University Press, Cambridge (1900)
10. West H. *Kinemetic analysis for the design and control of braced manipulators*. PhD thesis, Massachusetts Institute of Technology, 1986. Department of Mechanical Engineering.

[1] This optimization with quadratic objective function with linear constraints is convex. Therefore, the local minimum is the global minimum. Computation time on a PC is less than 1s.

[2] Note that a transformation of the compliance matrix (Eq. (11) in [1]) is required if the task frame origin and the location where the tool contacts the workpart are not collocated. In this example, because the task frame origin is located at the location of tool–workpart contact, no transformation is required.